Endothelial Cell Morphology in Areas of *In Vivo* Evans Blue Uptake in the Aorta of Young Pigs

II. Ultrastructure of the Intima in Areas of Differing Permeability to Proteins

R. G. Gerrity, PhD, Mary Richardson, PhD, J. B. Somer, PhD, F. P. Bell, PhD, and C. J. Schwartz, MD

The fine structure of the intima of the pig aortic arch is described for areas of spontaneously differing *in vivo* endothelial permeability, as demarcated by uptake of the protein-binding azo dye Evans blue. Areas of enhanced permeability (blue areas) consistently show a variety of features not observed in areas devoid of dye accumulation (white areas). The subendothelial space of blue areas is markedly thickened and edematous, containing collagen, elastic tissue elements, and undifferentiated cells dispersed in an amorphous floccular matrix of low electron density. Endothelial cells in blue areas are generally cuboidal, with relatively short, frequently vacuolated junctions. In contrast, endothelial cells from white areas are flat and elongate, with long intercellular junctions exhibiting many interdigitations. Cytoplasmic differences include a well-developed rough endoplasmic reticulum and more frequent lysosomal bodies in blue areas and a prominent Golgi apparatus in the endothelium of white areas. Additionally, endothelial cell injury or death with and without denudation occurs with a significantly greater frequency in blue relative to white areas. An endothelial glycocalyx is some threefold thicker over the surface of white relative to blue areas. It is concluded that neither endothelial structure nor function are homogeneous within the aortic arch of the young pig and that areas of spontaneously differing permeability to proteins are associated with a spectrum of alterations in endothelial and intimal morphology. (Am J Pathol 89:313–334, 1977)

THERE IS NOW EVIDENCE that aortic endothelial permeability to proteins such as ^{131}I-albumin and ^{131}I-fibrinogen is not homogeneous and that areas of spontaneously occurring greater permeability are readily demarcated *in vivo* in the young pig by their uptake of the protein-binding azo dye evans blue.[1-3] Such areas of dye uptake and enhanced permeability in the aortic arch exhibit an increased rate of endothelial cell turnover [4] and a number of differences in *en face* endothelial morphology relative to areas of no dye accumulation.[5] Additionally, areas of dye

From the Department of Atherosclerosis and Thrombosis, Research Division, The Cleveland Clinic Foundation, Cleveland, Ohio, and the Department of Pathology, Faculty of Health Sciences, McMaster University, Hamilton, Ontario, Canada.

Supported by Grant MT-3067 from the Medical Research Council of Canada and by the Ontario Heart Foundation and the Cleveland Clinic Foundation.

Accepted for publication June 27, 1977.

Address reprint requests to Dr. R. G. Gerrity, Department of Atherosclerosis and Thrombosis Research, The Cleveland Clinic Foundation, 9500 Euclid Avenue, Cleveland, OH 44106.

uptake have been shown to be more susceptible to endothelial injury induced by intravenous endotoxin.[6,7] To clarify the light microscopic findings and also to explore the possible structural correlates of areas of spontaneously differing aortic endothelial permeability to proteins, an ultrastructural study of the aortic intima was undertaken.

Materials and Methods

Eighteen Yorkshire-Landrace pigs, 8 to 10 weeks old, weighing 15 to 25 kg, were fed a commercial pelleted diet (Purina Hog Chow, Ralston-Purina Co., Canada) and water *ad libitum*.

The animals were anesthetized by an intravenous injection of sodium pentobarbitol (Diabutal, Diamond Laboratories, Des Moines, Iowa), and the jugular vein and carotid artery were exposed and cannulated. Fifty milliliters of Evans blue (Baker Chemical Co., C.I. 23860) were introduced through the jugular cannula. Evans blue was prepared as a 0.5% solution in sterile 0.85% saline and filtered through a 0.2-μ Gelman Metricel filter prior to use. In control experiments, 50 ml of isotonic sterile saline was injected in lieu of Evans blue.

Three hours after the Evans blue or saline injections, the animals were lightly reanesthetized as above, the carotid cannula was connected to a pressure perfusion apparatus, and systolic blood pressure measured. The left femoral artery was exposed and cut, and the pig was bled for 2 to 4 minutes, during which time 500 ml of oxygenated, heparinized Krebs-Ringer-bicarbonate solution (isotonic with pig serum at 37 C, pH 7.2) was perfused through the carotid cannula at systolic pressure. This was immediately followed by perfusion of 1 liter of fixative at systolic blood pressure and a temperature of 37 C. Initially, three fixatives were used: a) Karnovsky's fixative containing 2% paraformaldehyde and 2% glutaraldehyde in 0.1 M sodium cacodylate buffer, pH 7.35, 900 mOsm;[8] b) 2% glutaraldehyde, 0.1 M sodium cacodylate, pH 7.35, 440 mOsm; c) 1% glutaraldehyde, 0.1 M sodium cacodylate, pH 7.35, 300 mOsm. (The 2% glutaraldehyde fixative resulted in the most consistent and optimal fine structural preservation and was used in all subsequent studies.) After perfusion, the aortas were removed intact and opened longitudinally along the ventral surface while immersed in fixative.

Blue and white areas from each animal were mapped on a standardized aortic diagram, and 1-cu-mm blocks were excised from both blue and white sites in the aortic arch using a razor blade. In 2 control animals given saline, the blocks were taken from sites which were consistently blue or white in other pigs (Figure 1). All tissue blocks were fixed at room temperature for a further 6 hours, washed for 1 hour in two changes of 0.1 M sodium cacodylate buffer, pH 7.35, containing 7.5% sucrose and 0.5 mg/ml $CaCl_2$, then postfixed in 1% osmium tetroxide [9] at 4 C for 1.5 hours. In addition, aortic samples from both blue and white areas from 5 pigs injected with Evans blue and 1 control pig injected with saline were stained with ruthenium red [10] to demonstrate the glycocalyx layer on the luminal surface of the endothelium. The blocks were then dehydrated in ethanol, embedded in Spurr's resin, and sectioned on a Reichert ultramicrotome. Ultrathin sections were collected on uncoated 200-mesh copper grids, stained with 5% methanolic uranyl acetate followed by lead citrate,[11] and examined in a Philips 301 electron microscope.

For scanning electron microscopy, samples of both blue and white areas were fixed and dehydrated as above, then critical point dried from CO_2 in a Bomar SPC-500 EX critical point dryer. They were then mounted on specimen pegs and coated with gold/palladium (60:40) in an Edwards vacuum coating unit equipped with a rotary specimen holder prior to examination in an AMR-1000 scanning electron microscope.

Silver-nitrate-stained endothelial Häutchen preparations were produced as described previously.[4,5]

Results

The pattern of *in vivo* Evans blue uptake observed in this series of experiments was similar to that already described in earlier studies.[5,12] Numbers and sites of sampling of areas of dye accumulation (blue areas) and areas of no dye accumulation (white areas) are shown diagrammatically in Text-figure 1. A total of 182 and 174 tissue blocks were examined from blue and white areas in the aortic arch, respectively, as well as 70 blocks from white areas in the upper thoracic aorta.

Under the conditions of perfusion fixation employed in these studies, the elastic laminae showed no significant undulation. Consistently good preservation of ultrastructural detail was obtained in both intimal and medial components.

Endothelial Cell Shape

Endothelial cells derived from areas devoid of dye accumulation (white areas) appeared consistently flattened and elongated, with considerable overlap of adjacent cells (Figure 1), while in blue areas they were more cuboidal, with little or no cellular overlap (Figure 2). These consistent differences in endothelial cell configuration are associated with a number of differences in the intercellular junctions which are described in detail subsequently. In addition to the overall differences in cell shape, endothelial cytoplasmic flaps or projections into the lumen were observed more frequently in blue (Figure 2) than in white areas. These projections, often of considerable length and complexity, were commonly located at junctional complexes, often overlying the luminal aspect of the junction (Figure 3).

Endothelial Cell Organelles

On a qualitative basis, both the structure and frequency of a number of cellular organelles—including mitochondria, nucleoli, free ribosomes, pinocytotic vesicles, cytoplasmic filaments, and microtubules—appeared similar in endothelial cells from blue and white areas. Although differences in the frequency of the above organelles may be present, such differences could not be ascertained without quantitation.

In contrast, however, definite differences in the prominence and development of the rough endoplasmic reticulum (RER), Golgi apparatus, and lysosomal bodies were noted between blue and white areas. The RER was more prominent in endothelial cells of blue areas (Figure 4), although it exhibited shorter profiles than those seen in white areas (Figure 5). Of particular interest is the observation that the Golgi apparatus was consistently well developed in the endothelium of white areas (Figure 5),

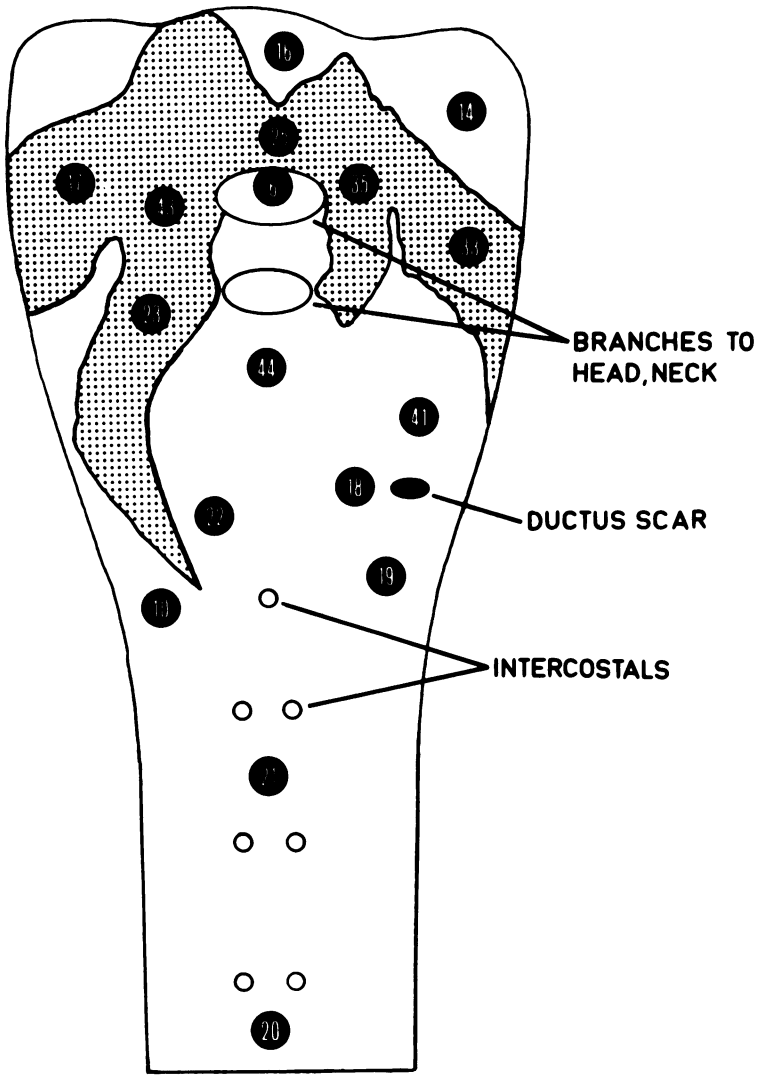

TEXT-FIGURE 1—Schematic diagram of pig aorta arch. *Dotted region* represents typical area of Evans blue uptake (produced by overlying transparencies of the aortas of the 18 pigs used in these experiments). Numbers in circles represent the numbers of electron microscopy blocks cut and examined from each site.

whereas it was rarely seen in endothelial cells from blue areas (Figure 6). A variety of inclusions, probably lysosomal in nature, was observed in the endothelium of both areas. Such inclusions consistently occurred in greater numbers in blue areas (Figure 6). They exhibited a variable density and in some instances were multivesicular.

Pinocytotic vesicles and caveoli were present on all surfaces of endothelial cells in both blue and white areas (Figures 4, 5, 7, and 8). The size and electron density of vesicles was similar in both areas. Some vesicles and caveoli in both blue and white areas contained varying amounts of ruthenium red–staining material, while other vesicles at a similar distance from the plasma membrane contained no such material (Figure 7). The ruthenium red–stained material within vesicles and caveoli appeared morphologically similar to that comprising the glycocalyx layer described subsequently. Although some apparent fusion of vesicles was observed (Figures 7 and 8), no patent channels or chains of vesicles extending across the endothelium were seen in blue or white areas.

Junctions

Although the general architecture of junctions between endothelial cells as seen in this study was similar to that observed in other large arteries, considerable focal variation in junctional morphology was observed between endothelial cells of blue and white areas. Associated with the differences in endothelial cell shape described above, most junctions in white areas were elongated and tortuous, with many interdigitations (Figure 8). By contrast, the more cuboidal endothelial cells of blue areas formed shorter, less complex, end-to-end junctions, with little or no interdigitation or cellular overlap (Figure 9). Such junctions frequently exhibited a marked segmental dilatation or vacuolation (Figures 4 and 9). Tight junctions were sometimes observed adjoining dilated segments and were frequently observed between endothelial cells in both blue and white areas.

Subendothelial Space

The subendothelial space, although variable, was consistently and strikingly thicker in blue (Figure 2) than in white (Figure 1) areas. The difference in thickness of the subendothelial space can best be appreciated by comparing Figures 1 and 2. In Figure 1 (from a white area), the internal elastic lamina is clearly evident, delineating the subendothelial space some 7 to 8 μ below the endothelium. Figure 2 (from a blue area) is shown at nearly half the magnification of Figure 1. The internal elastic lamina is not visible at a depth of 30 to 35 μ below the endothelium. In white areas, the endothelium was closely applied either to the developing internal elastic lamina or to modified smooth muscle cells which lay parallel to the endothelial layer (Figures 1 and 10). In blue areas, the subendothelial space appeared markedly edematous, with variable amounts of collagen, elastic tissue, and microfibrils scattered in a back-

ground of floccular material of low electron density (Figure 2). Intimal cells in blue areas were seldom in close proximity to the endothelium and were either very elongate with numerous cytoplasmic processes (Figure 2) or ovoid in shape (Figure 6). In the former, the presence of myofilaments and dense bodies suggested a smooth muscle cell origin, while the latter more closely resembled blood-derived mononuclear cells (Figure 6). Both the above cell types contained frequent lysosome-like inclusions (Figures 2 and 6). In both blue and white areas the endothelial basement membrane was incomplete (Figures 3, 6, and 8).

Endothelial Glycocalyx

In sections stained with uranium and lead salts, a definite, though lightly-staining, fuzzy layer was observed on the luminal surface of endothelial cells from white areas (Figures 1 and 8). In contrast, this layer was barely perceptible or apparently absent over endothelial cells in blue areas (Figures 2–4). With ruthenium red staining, this difference in the thickness of the glycocalyx was accentuated. The glycocalyx in both areas had two components; a dense lamina closely applied to, or continuous with, the plasmalemmal membrane and, superficially, a layer of decreasing density exhibiting a finely fibrillar meshwork (Figures 11 and 13). Both components—the inner dense lamina and the superficial fibrillar meshwork—were each much thicker in white (Figure 11) than in blue (Figure 12) areas. Additionally, circular or oval structures of densely-stained material were conspicuous in the surface coat from white areas (Figure 11) but not from blue areas (Figure 12). The thickness of the glycocalyx was measured from twenty electron micrographs each of blue and white areas taken from ten tissue blocks from two standard sites (one blue, one white) in 5 animals. The mean glycocalyx thickness in blue areas was found to be 130 Å, as compared to 440 Å in white areas (cf. Figures 11 and 12), a statistically significant difference ($P < 0.05$). Additionally, the amount of ruthenium present in the glycocalyx was measured using energy dispersive analysis of x-rays and was found to be threefold greater in white than in blue areas (Figure 13), a finding consistent with the thickness measurements.

Endothelial Cell Injury

A spectrum of changes consonant with endothelial cell injury—ranging from minor morphologic alterations to overt cell death—was consistently observed in blue areas but rarely in white areas. Changes noted include disruption of mitochondrial cristae with peripheral condensation, mitochondrial swelling, and a general loss of cytoplasmic organelles (Figure

14), as well as prominent cytoplasmic and junctional vacuolation (Figures 3, 4, 9, and 14) and ultimately cellular death and sloughing with or without disruption. In some instances, dead or severely injured cells were partially or completely lifted into the lumen. Highly vacuolated cells with numerous cytoplasmic extensions exhibiting a greater electron density than adjacent endothelial cells were sometimes observed in these regions (Figure 15). Because of their density and vacuolation, it was difficult to determine whether these cells were degenerate endothelial cells or attenuated, degranulated platelets. However, when viewed in the scanning electron microscope, adherent platelets were observed individually and were sometimes associated with erythrocytes, leukocytes, and fibrin strands, forming a microthrombus (Figure 16). These were not observed in white areas. Dead or injured cells characteristically exhibited a diffuse cytoplasmic staining with ruthenium red (Figure 17) in addition to the characteristic surface staining. The frequency of injured or dead cells in the endothelium was not assessed by electron microscopy in relation to the number of normal cells. However, in silver-nitrate–stained Häutchen preparations of endothelium in which injured or dead cells show intense silver staining (Figure 18), such cells were found to occur with a significantly greater frequency in blue (2.91%) than in white (0.71%) areas ($P < 0.001$). These frequencies were determined by counting a random sample of 1427 and 1296 cells from blue and white areas, respectively.

Control Experiments

Because of the possibility that the presence of Evans blue might itself result in changes in the endothelium, subendothelial space, and glycocalyx, two control studies were undertaken in which saline alone was injected into the animals and the sites customarily showing dye uptake and no dye uptake were removed for study. In no instance in these presumptive blue and white areas did the ultrastructural morphology differ from those experiments in which Evans blue had been injected, indicating that the presence of Evans blue alone is not responsible for the blue–white differences observed.

Discussion

In this study, we have described and compared the fine structure of the intima of the aortic arch in the normal young pig derived from areas of spontaneously differing *in vivo* endothelial permeability to proteins. Areas of greater permeability were consistently demarcated in the aortic arch by their uptake of the protein-binding azo dye Evans blue [1-3] and have been shown to exhibit a number of additional features; these include

the following: differences in *en face* endothelial morphology;[5] an increased endothelial cell turnover as measured by nuclear ^{3}H-thymidine incorporation;[4] a greater susceptibility to endotoxin-induced endothelial injury;[6,7] an enhanced uptake and turnover of ^{3}H-unesterified cholesterol;[12,13] together with a variety of differences in lipid biosynthesis.[14-17] In addition, a greater accumulation of cholesterol in the aortic intima in blue relative to white areas has been demonstrated in cholesterol-fed pigs,[18,19] raising the possibility that such foci might be areas of early atherogenesis, as indicated by Fry.[20] Notwithstanding the possible relevance of such areas to the process of atherogenesis, the Evans blue model is of intrinsic biologic interest in terms of aortic endothelial permeability, and the remaining discussion will be directed toward this end.

In the present study, pinocytotic or plasmalemmal vesicles were commonly observed in endothelial cells of both blue and white areas, and caveoli were observed on the luminal, abluminal, and junctional surfaces. No differences in the frequency or structure of these organelles were apparent between the two areas. However, some prominent differences in the morphology of intercellular junctions were consistently observed between blue and white areas. Specifically, most junctions in white areas were complex, elongated, and tortuous, with numerous interdigitations, while in blue areas the junctions were shorter, end-to-end, and frequently exhibited a prominent segmental dilatation or vacuolation. Tight junctions or zonulae occludentes,[21] occurred in both blue and white areas, and in neither blue nor white areas did we find gaping spaces between normal endothelial cells. Both pinocytotic vesicles and intercellular junctions have been implicated in the transendothelial transport of molecules in large arteries [22-27] and in capillaries.[28-33] Since we were unable to find qualitative differences in the frequency of vesicles in blue and white areas, it is unlikely that the greater permeability of blue areas can be explained solely on the basis of a numerical difference in vesicles. It is feasible that the longer interdigitating junctions found in white areas might be associated with a less rapid molecular transport, relative to the shorter junctions in blue areas. Additionally, it is difficult to envisage how the segmental dilatation of intercellular junctions in blue areas might be responsible for enhanced endothelial permeability. Such junctional dilatations are clearly not analogous to the gap junctions described by Hüttner, Boutet, and More [25] and, in some instances, may be another manifestation of endothelial cellular injury, as discussed below.

Of particular interest is the demonstration in blue areas in the normal young pig aorta of a wide spectrum of changes consistent with endothelial cellular injury or death, including loss of cytoplasmic density, degeneration of organelles, cytoplasmic vacuolation, indentation of nuclear mem-

branes, chromatin aggregation, and the formation of cytoplasmic surface projections. Additionally, partial or complete endothelial cell ablation was frequently observed in blue areas. Light microscopy on silver-stained Häutchen preparations revealed foci of intense silver staining sharply delineated by silver-stained cellular boundaries within the confines of blue areas. These have been interpreted as being injured or dead cells,[5] an interpretation reinforced by the present ultrastructural observations that cells demonstrating severe cytoplasmic degeneration also show a marked cytoplasmic uptake of ruthenium red. A similar, though more extensive, pattern of intense silver staining has been observed in blue areas of the dog aorta after a single intravenous injection of endotoxin and has been correlated ultrastructurally with endothelial cell injury, denudation, and platelet adherence.[7,34] This demonstration of cell injury and death is also consistent with the greater endothelial cell turnover observed in blue areas.[4] Another facet of endothelial injury relates to the presence of electron-dense vacuolated cells in blue areas, with normal endothelial cells adjacent to them. The possibility exists that these are portions of damaged endothelial cells or, alternatively, that they are attenuated degranulated platelets. The latter possibility is supported by the scanning electron microscopic demonstration of platelet adherence and occasional microthrombi in blue areas. Such adherence may reflect the propensity of platelets to interact with exposed connective tissue components, or, alternatively (as suggested by Mustard *et al.*[35]), platelets near or in contact with the endothelium might cause or enhance endothelial injury through the release of lysosomal enzymes, serotonin, and histamine. The relative contribution of platelets to the endothelial damage observed in this study remains uncertain. However, these composite findings emphasize that in the overtly normal aorta, foci of endothelial injury or death are present within the larger confines of areas of Evans blue accumulation, and, as suggested earlier,[4,5] it is possible that the endothelial injury is mediated directly or indirectly by hemodynamic stress.

Focal endothelial cell injury or death, as observed in this study, might feasibly result in the development of a number of physical defects in the endothelium which could function as "ultralarge pores" and thus contribute to the enhanced permeability of blue areas. These defects occur with a greater frequency in blue (2.91%) than in white (0.71%) areas. Whether the observed differences in frequency of such defects can account for the greater endothelial permeability of blue areas or whether platelets overlying such defects are themselves impermeable to plasma constituents remains uncertain. Current studies with a variety of molecular probes should clarify the relative magnitude of this avenue of transendothelial transport, which cannot be evaluated on the basis of the ultrastructural

observations alone. Clearly, however, spontaneously occurring endothelial injury is an additional factor which needs careful consideration in studies and models of large artery permeability.

A conspicuous feature of blue areas is the greatly widened subendothelial space, within which a floccular material of low electron density is the major component. The subendothelial space in blue areas has the appearance of intimal edema and has been so interpreted by Packham *et al.*[1] Widening of the subendothelial space has been described by others,[36-38] particularly in relation to aortic branching sites. Schwartz and Benditt [24] noted a threefold variation in the thickness of the subendothelial space in the rat aorta, a variation which might be explained by their sampling of areas corresponding to "blue" and "white" foci as in the present study. The thickened edematous subendothelial space described in blue areas in the present study does not appear equivalent to the diffuse developmental thickening of the intima described in rats by Gerrity and Cliff [39] and in man,[40] nor is it analogous to the thickening associated with experimental hypertension in the rat aorta in which polymerized fibrin was observed.[23] Whether the increased endothelial permeability observed in blue areas [2,3] results in or is the result of subendothelial thickening has yet to be determined. A greater secretion of mucopolysaccharides in these regions may contribute to the thickened subendothelial space, which is also metachromatic with toluidine blue.

Of interest in this study is the consistent observation that the surface-associated mucopolysaccharide coat, or glycocalyx,[41] is some threefold thicker over the endothelium of white areas than blue areas. A surface-associated mucopolysaccharide layer on or attached to the plasmalemmal membrane has been observed in relation to a wide variety of cells,[10,41-43] while a vascular endothelial glycocalyx has been described by a number of investigators using ruthenium red and concanavalin A.[44-47] It has been suggested that this surface layer or glycocalyx may be a physiologically important codeterminant of a number of cellular or membrane properties including permeability, filtration, selective binding, ion exchange, and cell adhesion.[10,41,42] Further, the presence of ruthenium red–staining material within pinocytotic vesicles has been noted both in this study and by others,[44,45] suggesting a possible role of the glycocalyx in vesicular transport.[45] Revel and Ito [48] have suggested that this surface layer can be considered along with the plasma membrane as a functional complex to which the term *greater membrane* may be applied. Notwithstanding the apparent nonspecificity of ruthenium red as a mucopolysaccharide stain,[49] its use in this study has been to facilitate visualization and quantitation of the differences in thickness of the glycocalyx between blue and white

areas, a difference which is, however, visible using conventional electron-dense stains.

Because of its striking correlation in the aortic arch with areas of differing permeability, it is indeed tempting to suggest that the thicker glycocalyx in white areas might be responsible, at least in part, for the lesser endothelial permeability of these areas to plasma proteins. It is also possible that the thicker glycocalyx, by modifying the nature or extent of the contact of circulating lipoproteins with the plasmalemmal membrane itself, might also interfere with the physicochemical exchange of unesterified cholesterol, thus at least partially accounting for the greater uptake of ^{3}H-unesterified cholesterol demonstrated in blue areas.[12,13] Whether differences in the glycocalyx reflect a response to focal differences in hemodynamic stress or whether the glycocalyx influences vesicular transport are issues which have yet to be clarified. However, it is interesting to note that experimental hypercholesterolemia has been associated with both enhanced aortic endothelial permeability to albumin [50,51] and a thinning of the glycocalyx.[47] Presumably, the components of the glycocalyx are synthesized in the Golgi apparatus,[52] which has long been implicated in mucopolysaccharide synthesis.[53] It is, therefore, interesting to contrast the number of well-developed Golgi apparatuses observed in white areas with their scarcity in blue areas in the present study.

A number of differences in endothelial organelles were observed in addition to the more prominent and well-developed Golgi apparatus in white areas. There is a greater development of the rough endoplasmic reticulum and a more frequent appearance of lysosomal bodies in blue areas than in white areas. The greater frequency and development of lysosomes and RER in blue areas may be a reflection of greater hemodynamic stress and continuing endothelial cell injury and repair analogous to the increased lysosomal content of arterial smooth muscle cells described in experimental hypertension.[54-56]

In summary: Structural differences in the endothelial cell layer may account for the observed blue–white differences in permeability to proteins,[2,3] but they are unlikely to account for the variety of metabolic differences observed between blue and white areas,[14-17] differences which in all probability relate to the large smooth muscle cellular mass rather than to the endothelium itself. However, such medial metabolic differences may themselves be secondary to differences in endothelial structure which result in a differing influx of plasma constituents.

References

1. Packham MA, Rowsell HC, Jørgensen L, Mustard JF: Localized protein accumulation in the wall of the aorta. Exp Mol Pathol 7:214–232, 1967

2. Bell FP, Adamson IL, Schwartz CJ: Aortic endothelial permeability to albumin: Focal and regional patterns of uptake and transmural distribution of ^{131}I-albumin in the young pig. Exp Mol Pathol 20:57–68, 1974
3. Bell FP, Gallus AS, Schwartz CJ: Focal and regional patterns of uptake and the transmural distribution of ^{131}I-fibrinogen in the pig aorta in vivo. Exp Mol Pathol 20:281–292, 1974
4. Caplan BA, Schwartz CJ: Increased endothelial cell turnover in areas of in vivo Evans blue uptake in the pig aorta. Atherosclerosis 17:401–417, 1973
5. Caplan BA, Gerrity RG, Schwartz CJ: Endothelial cell morphology in focal areas of in vivo Evans Blue uptake in the young pig aorta. I. Quantitative light microscopic findings. Exp Mol Pathol 21:102–117, 1974
6. Gerrity RG, Richardson M, Caplan BA, Cade JF, Hirsh J. Schwartz CJ: Endotoxin-induced vascular endothelial injury and repair. II. Focal injury, en face morphology, [^{3}H] thymidine uptake and circulating endothelial cells in the dog. Exp Mol Pathol 24:59–69, 1976
7. Gerrity RG, Richardson M, Schwartz CJ: Endotoxin-induced vascular endothelial injury and repair. III. Ultrastructural observations on the aorta and pulmonary artery of the dog. Exp Mol Pathol (In press)
8. Millonig G, Bosco M: Some remarks on paraformaldehyde as fixative. J Cell Biol 35:177A–178A, 1967
9. Caulfield JB: Effects of varying the vehicle for OsO_4 in tissue fixation. J Biophys Biochem Cytol 3:827–830, 1957
10. Luft JH: Ruthenium red and violet. II. Fine structural localization in animal tissues. Anat Rec 171:369–416, 1971
11. Venable JH, Coggeshall RA: A simplified lead citrate stain for use in electron microscopy. J Cell Biol 25:407–408, 1965
12. Somer JB, Schwartz CJ: Focal [^{3}H] cholesterol uptake in the pig aorta. Atherosclerosis 13:293–304, 1971
13. Somer JB, Schwartz CJ: Focal [^{3}H] cholesterol uptake in the pig aorta. II. Distribution of ^{3}H-cholesterol across the aortic wall in areas of high and low uptake in vivo. Atherosclerosis 16:377–388, 1972
14. Somer JB, Bell FP, Schwartz CJ: Focal differences in lipid metabolism of the young pig aorta: Synthesis from [1-^{14}C] acetate and [U-^{14}C] glucose in vitro. Atherosclerosis 20:11–21, 1974
15. Somer JB, Schwartz CJ: Focal differences in lipid metabolism of the young pig aorta. II. Synthesis from [2-^{14}C] ethanolamine and [1, 2-^{14}C] choline. Atherosclerosis 20:507–516, 1974
16. Somer JB, Gerrity RG, Schwartz CJ: Focal differences in lipid metabolism of the young pig aorta. III. Influence of insulin on lipogenesis from [1-^{14}C] acetate. Exp Mol Pathol 24:1–12, 1976
17. Somer JB, Schwartz CJ: Focal differences in lipid metabolism of the young pig aorta. IV. Influence of insulin and epinephrine on lipogenesis from [^{14}C] U-glucose. Exp Mol Pathol 24:129–141, 1976
18. Day AJ, Bell FP, Schwartz CJ: Lipid metabolism in focal areas of normal-fed and cholesterol-fed pig aorta. Exp Mol Pathol 21:179–193, 1974
19. Bell FP, Day AJ, Gent M, Schwartz CJ: Differing patterns of cholesterol accumulation and ^{3}H-cholesterol influx in areas of the cholesterol-fed pig aorta identified by Evans blue dye. Exp Mol Pathol 22:366–375, 1975
20. Fry DL: Responses of the arterial wall to certain physical factors. Atherogenesis: Initiating Factors. Ciba Foundation Symposium, No. 12. New York, Excerpta Medica Foundation, 1973, pp 93–125
21. Farquhar MG, Palade GE: Junctional complexes in various epithelia. J Cell Biol 17:375–412, 1962

22. Florey L, Sheppard BL: The permeability of arterial endothelium to horseradish peroxidase. Proc R Soc Lond [Biol] 174:435–443, 1970
23. Hüttner I, More RH, Rona G: Fine structural evidence of specific mechanism for increased endothelial permeability in experimental hypertension. Am J Pathol 61:395–412, 1970
24. Schwartz SM, Benditt EP: Studies on aortic intima. I. Structure and permeability of rat thoracic aortic intima. Am J Pathol 66:241–264, 1972
25. Hüttner I, Boutet M, More RH: Gap junctions in arterial endothelium. J Cell Biol 57:247–252, 1973
26. Hüttner I, Boutet M, More RH: Studies on protein passage through arterial endothelium. I. Structural correlates of permeability in rat arterial endothelium. Lab Invest 28:672–677, 1973
27. Hüttner I, Boutet M, Rona G, More RH: Studies on protein passage through arterial endothelium. III. Effect of blood pressure levels on the passage of fine structural protein tracers through rat arterial endothelium. Lab Invest 29:536–546, 1973
28. Majno G: Ultrastructure of the vascular membrane. Handbook of Physiology, Section 2: Circulation, Vol 3. Edited by WF Hamilton. Baltimore, Williams & Wilkins Co., 1965, pp 2293–2375
29. Karnovsky MJ: The ultrastructural basis of capillary permeability studied with peroxidase as a tracer. J Cell Biol 35:213–236, 1967
30. Bruns RR, Palade GE: Studies on blood capillaries. II. Transport of ferritin molecules across the wall of muscle capillaries. J Cell Biol 37:277–299, 1968
31. Clementi F, Palade GE: Intestinal capillaries. I. Permeability to peroxidase and ferritin. J Cell Biol 41:33–58, 1969
32. Simionescu N, Simionescu M, Palade GE: Permeability of muscle capillaries to exogenous myoglobin. J Cell Biol 57:424–452, 1973
33. Simionescu N, Simionescu M, Palade GE: Permeability of muscle capillaries to small heme-peptides: Evidence for the existence of patent transendothelial channels. J Cell Biol 64:586–607, 1975
34. Gerrity RG, Caplan BA, Schwartz CJ, Richardson M: Endotoxin-induced vascular endothelial injury in the dog. Proceedings of the Eighth International Congress on Electron Microscopy, Canberra, Australia, Vol II. Netley, S. Australia, The Griffin Press 1974, pp 552–553
35. Mustard JF, Jørgensen L, Packham MA: Formed elements as a source of vascular injury. Thromb Diath Haemorrh Suppl 40:137–144, 1970
36. Duff GL, McMillan GC, Ritchie AC: The morphology of early atherosclerotic lesions of the aorta demonstrated by the surface technique in rabbits fed cholesterol. Am J Pathol 33:845–874, 1957
37. Stehbens WE: The renal artery in normal and cholesterol-fed rabbits. Am J Pathol 43:969–986, 1963
38. French JE: Atherosclerosis in relation to the structure and function of the arterial intima, with special reference to the endothelium. Int Rev Exp Pathol 5:253–353, 1966
39. Gerrity RG, Cliff WJ: The aortic tunica intima in young and aging rats. Exp Mol Pathol 16:382–402, 1972
40. Movat HZ, More RH, Haust MD: The diffuse intimal thickening of the human aorta with aging. Am J Pathol 34:1023–1031, 1958
41. Bennett HS: Morphological aspects of extracellular polysaccharides. J Histochem Cytochem 11:14–23, 1963
42. Philpott CW: Functional implications of the cell surface: The plasmalemma and surface-associated polyanions. Ciba Found Study Group 32:109–122, 1968

43. Rambourg A: Morphological and histochemical aspects of glycoproteins at the surface of animal cells. Int Rev Cytol 31:57–114, 1971
44. Luft JH: Fine structure of capillary and endocapillary layer as revealed by ruthenium red. Fed Proc 25:1773–1783, 1966
45. Shirahama T, Cohen AS: The role of mucopolysaccharides in vesicle architecture and endothelial transport: An electron microscope study of myocardial blood vessels. J Cell Biol 52:198–206, 1972
46. Weber G, Fabbrini P, Resi L: On the presence of a concanavalin-A reactive coat over the endothelial aortic surface and its modifications during early experimental cholesterol atherogenesis in rabbits. Virchows Arch [Pathol Anat] 359:299–307, 1973
47. Bálint A, Veress B, Jellinek H: Modifications of surface coat of aortic endothelial cells in hyperlipemic rats. Pathol Eur 9:105–108, 1974
48. Revel J, Ito S: The Specificity of Cell Surfaces. Edited by BD Davis, L. Warren. Englewood Cliffs, N.J., Prentice-Hall, 211–234, 1967.
49. Copley AL, Scheinthal BM: Nature of the endothelial layer as demonstrated by ruthenium red. Exp Cell Res 59:491–492, 1970
50. Stefanovich V, Gore I: Cholesterol diet and permeability of rabbit aorta. Exp Mol Pathol 14:20–29, 1971
51. Bell FP, Adamson IL, Gallus AS, Schwartz CJ: Endothelial permeability: Focal and regional patterns of ^{131}I-albumin and ^{131}I-fibrinogen uptake and transmural distribution in the pig aorta. Proceedings of the Third International Symposium on Atherosclerosis, 1973. Edited by G Schettler, A Weizel. Berlin, Springer-Verlag, 1975
52. Rambourg A, Hernandez W, LeBlond CP: Detection of complex carbohydrates in the Golgi apparatus of rat cells. J Cell Biol 40:395–414, 1969
53. Neutra M, LeBlond CP: Synthesis of the carbohydrate of mucus in the Golgi complex as shown by electron microscope radioautography of goblet cells from rats injected with glucose-H^3. J Cell Biol 30:119–136, 1966
54. Wolinsky H, Goldfischer S, Schiller B, Kasak LE: Lysosomes in aortic smooth muscle cells: Effects of hypertension. Am J Pathol 73:727–734, 1973
55. Wolinsky H, Goldfischer S, Schiller B, Kasak LE: Modification of the effects of hypertension on lysosomes and connective tissue in the rat aorta. Circ Res 34:233–241, 1974
56. Wolinsky H, Goldfischer S, Daly MM, Kasak LE, Coltoff-Schiller B: Arterial lysosomes and connective tissue in primate atherosclerosis and hypertension. Circ Res 36:553–561, 1975

Legends for Figures

Figure 1—Low-power transmission electron micrograph of the intima from a white area in the pig aortic arch. Endothelial cells (*E*) are elongate and flat, with a prominent glycocalyx (*G*) on the surface facing the lumen(*L*). Scattered fragments of elastica (*EL*) and collagen (*C*) are visible in the subendothelial space (*SES*). The internal elastic lamina (*IEL*) has partially formed, and two smooth muscle-derived cells (*IC*) can be seen in the intima, as well as smooth muscle cells (*SM*) in the media. (Lead citrate and uranyl acetate, × 6000)

Figure 2—Similar to Figure 1, but from an blue area of dye uptake. Endothelial cells (*E*) are cuboidal in shape with frequent cytoplasmic extensions (*CE*) into the lumen (*L*). There is little cellular overlap between adjacent endothelial cells. The subendothelial space (*SES*) is greatly thickened and edematous, with more elastica (*EL*) and collagen (*C*) than is present in white areas (compare with Figure 1). Intimal cells (*IC*) are numerous, elongate and frequently contain lysosomes (*arrows*). The internal elastic lamina is not visible at this magnification. (Lead citrate and uranyl acetate, × 3200)

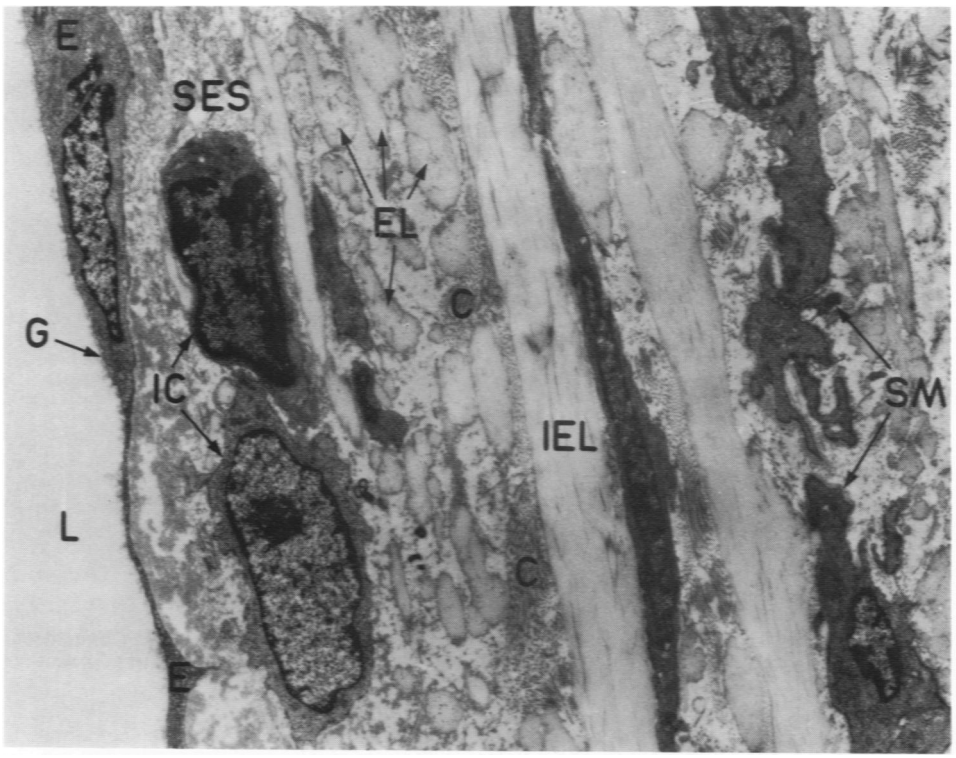

1

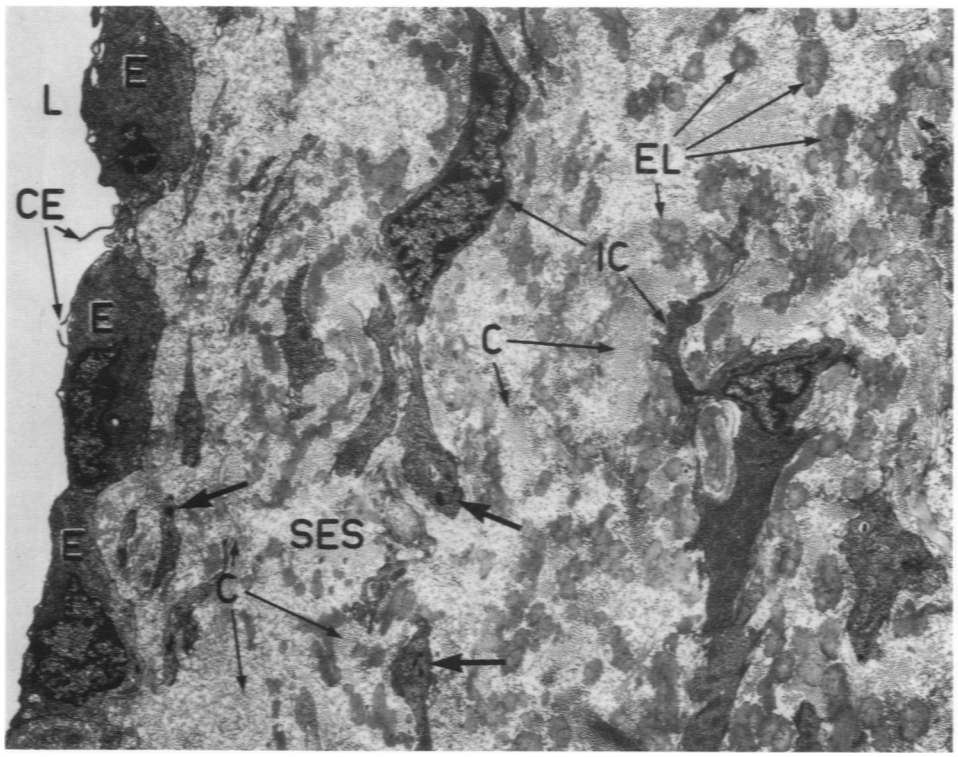

2

Figure 3—Electron micrograph of endothelium (*E*) from an area of dye uptake. Complex cytoplasmic processes (*arrows*) extend into lumen (*L*) at a junctional region (*J*), and adjacent cytoplasm is vacuolated (*V*). (Lead citrate and uranyl acetate, × 20,500)

Figure 4—Electron micrograph of endothelial cell cytoplasm from a blue area. Note segmental dilatation or vacuolation of junction and adjacent cytoplasm (*arrows*). Mitochondria (*M*) are present, as are numerous pinocytotic vesicles (*Ve*). Much of the cytoplasm is filled with free ribosomes and short profiles of rough endoplasmic reticulum (*ER*). Lumen (*L*) is at top. (Lead citrate and uranyl acetate, × 20,500)

Figure 5—As in Figure 4, but from a white area. Rough endoplasmic reticulum (*ER*) is not as prominent as in blue areas, but Golgi complexes (*G*) are well-developed. Mitochondria (*M*), vesicles (*Ve*), and numerous cytoplasmic filaments (*F*) are also visible. (Lead citrate and uranyl acetate, × 50,500)

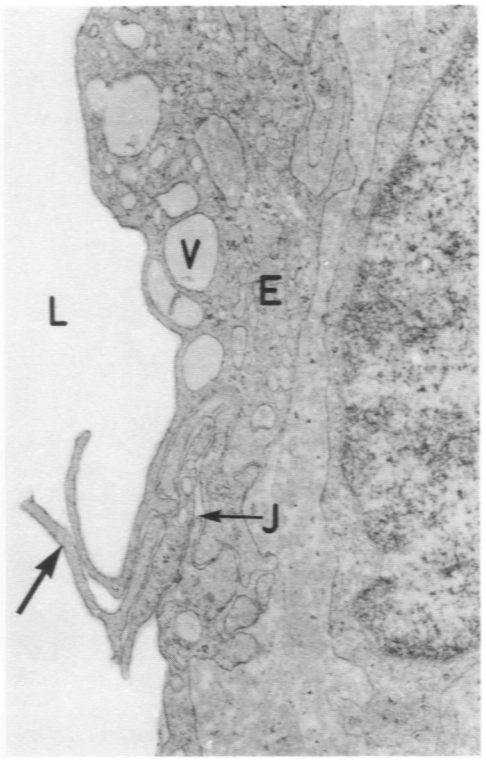

3

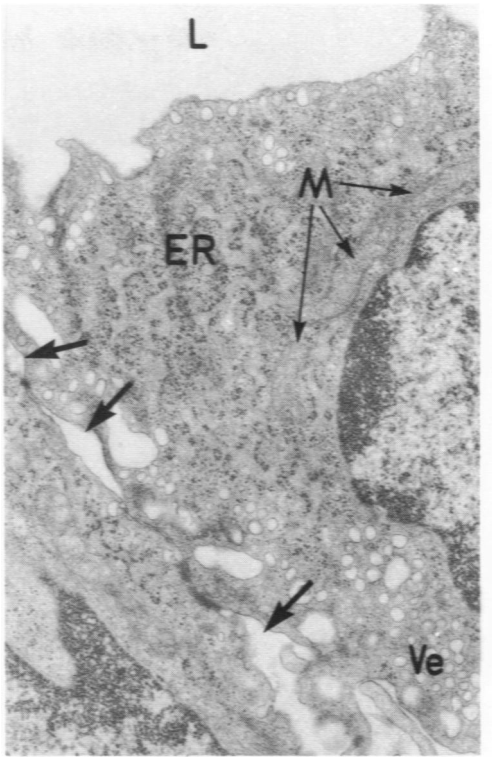

4

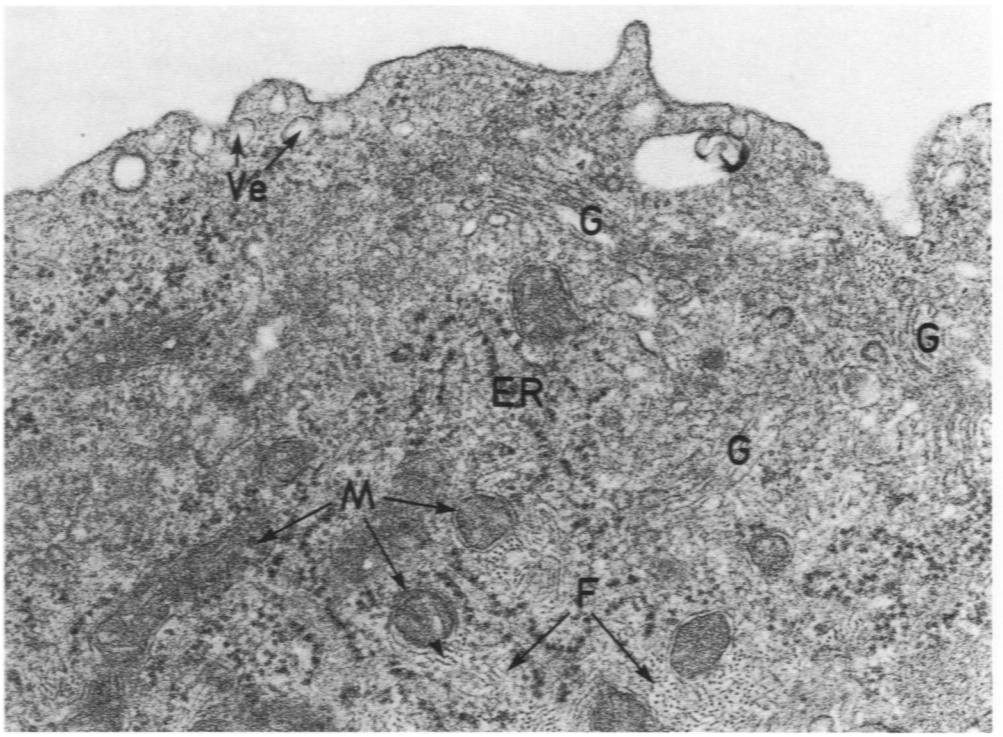

5

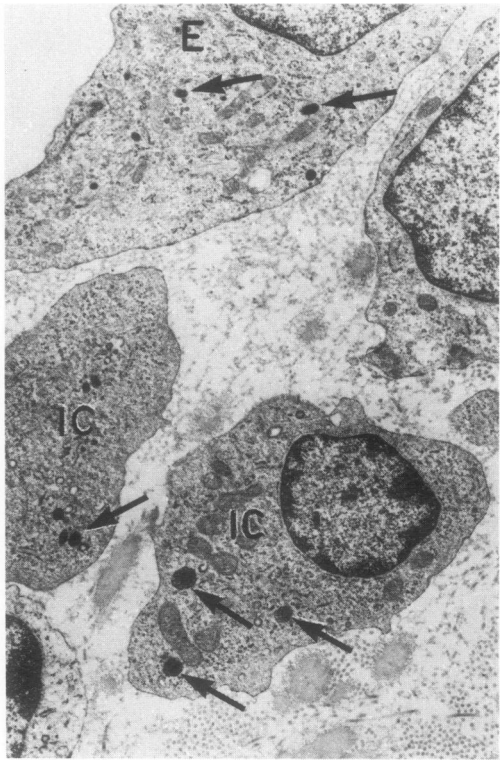

6

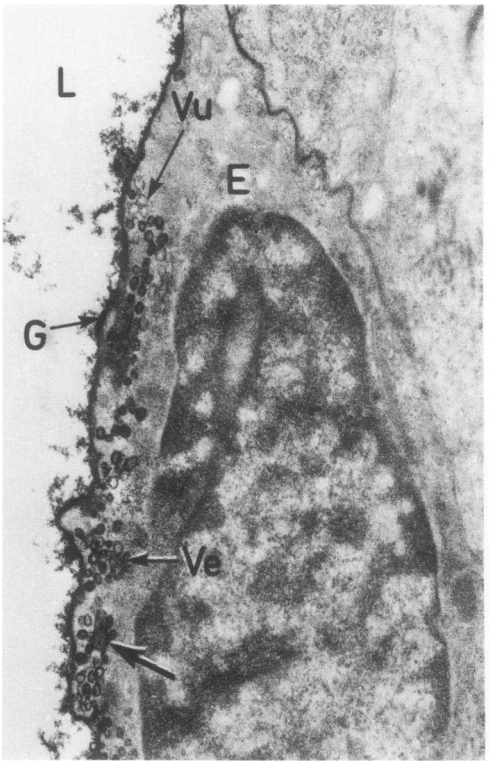

7

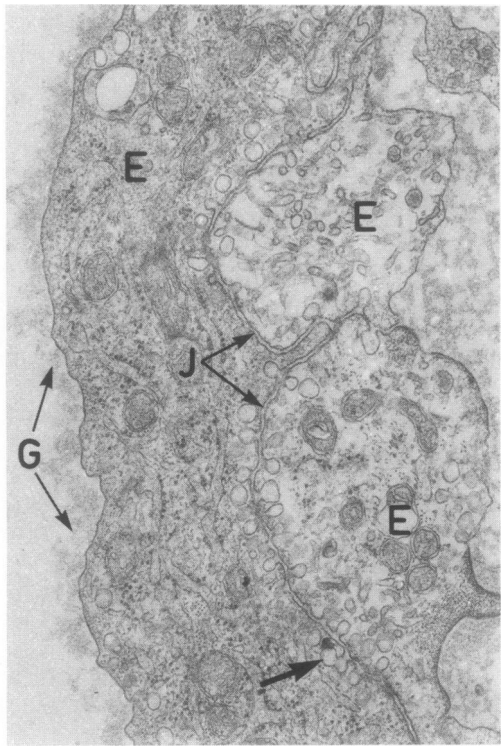

8

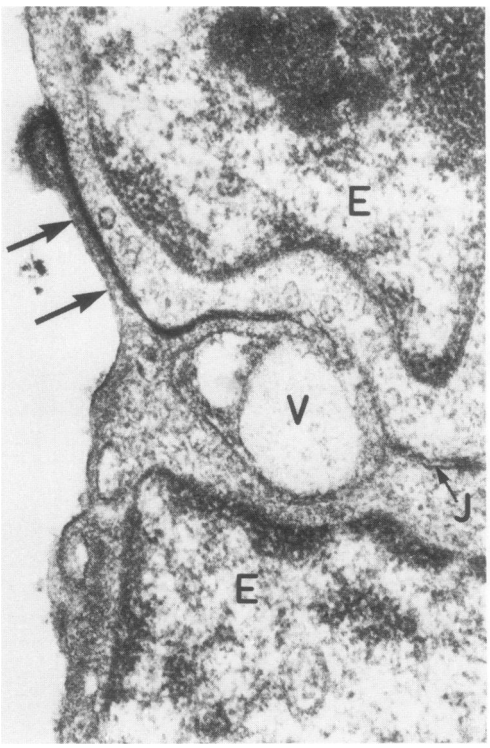

9

Figure 6—Electron micrograph of intima from a blue area. Both endothelial cells (*E*) and intimal cells (*IC*) contain numerous lysosome-like inclusions (*arrows*) of variable size and density. (Lead citrate and uranyl acetate, × 10,900) **Figure 7**—Electron micrograph of endothelium (*E*) from a blue area stained with ruthenium red. Note staining of glycocalyx layer (*G*) on surface of endothelium. Ruthenium red-stained material can be observed in some vesicles (*Ve*), while other vesicles at a similar distance from the lumen (*L*) are unstained (*Vu*). Fusion of vesicles can be observed (*arrows*). (Ruthenium red block-stained, × 20,200) **Figure 8**—Electron micrograph of complex interdigitating junction (*J*) typically found between endothelial cells (*E*) in a white area. Note also the prominent glycocalyx (*G*) and possible fusion of cytoplasmic vesicles (*arrow*). (Lead citrate and uranyl acetate, × 26,800) **Figure 9**—Electron micrograph of junction (*J*) typically seen in blue area endothelium. Endothelial cells (*E*) are cuboidal in shape, forming a short end-to-end junction with only slight cellular overlap (*arrows*). A large vacuole (*V*) is associated with the junction. Note absence of glycocalyx. (Ruthenium red block-stained, × 33,500)

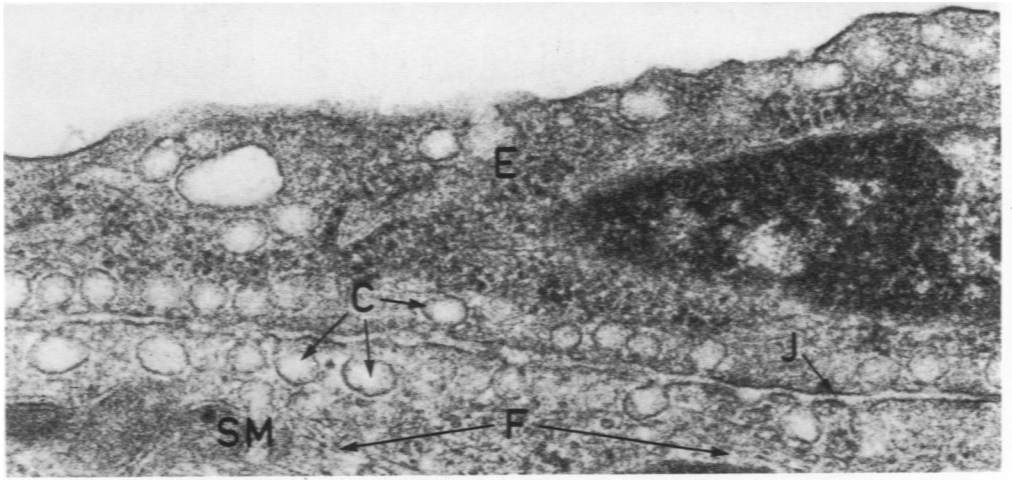

10

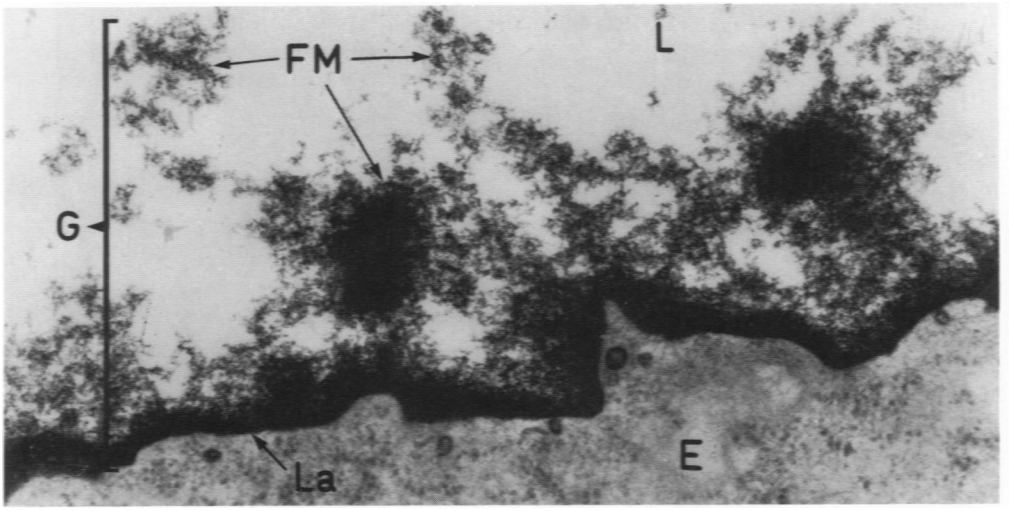

11

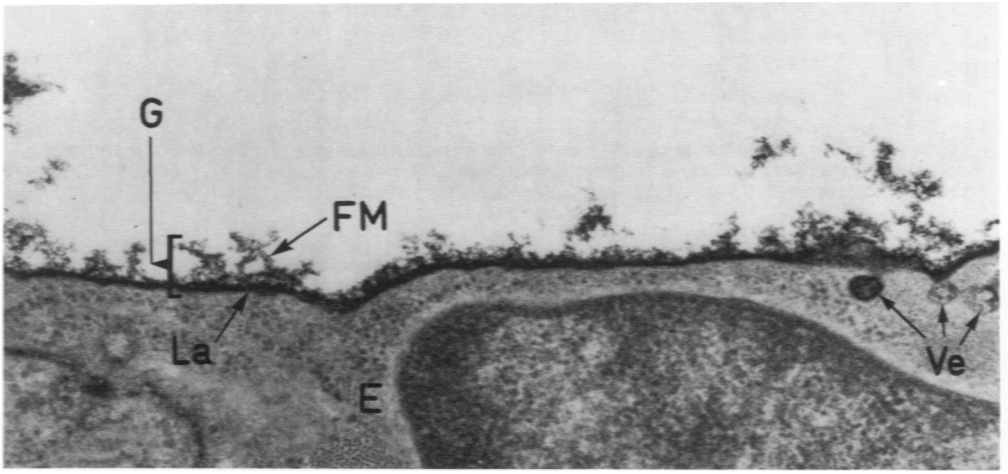

12

Figure 10—Electron micrograph of intima from a white area. Intimal smooth muscle–derived cell (*SM*) containing myofilaments (*F*) lies parallel and closely opposed to endothelium (*E*), forming a junctional region (*J*) into which caveolae (*C*) from both cells open. (Lead citrate and uranyl acetate, × 78,200) **Figure 11**—Endothelium (*E*) from a white area stained with ruthenium red to demonstrate the glycocalyx (*G*), which consists of a dense inner lamina (*La*) closely applied to the plasma membrane, and a superficial finely fibrillar meshwork (*FM*) extending into the lumen (*L*). Compare with Figure 12. (Ruthenium red block-stained, × 51,000) **Figure 12**—Endothelium (*E*) from a blue area stained with ruthenium red. Glycocalyx (*G*) is visibly thinner than that in white areas (compare with Figure 11 at same magnification), both in terms of the dense inner lamina (*La*) and the fibrillar meshwork (*FM*). Vesicles (*Ve*) show variable degrees of staining. (Ruthenium red block-stained, × 51,000)

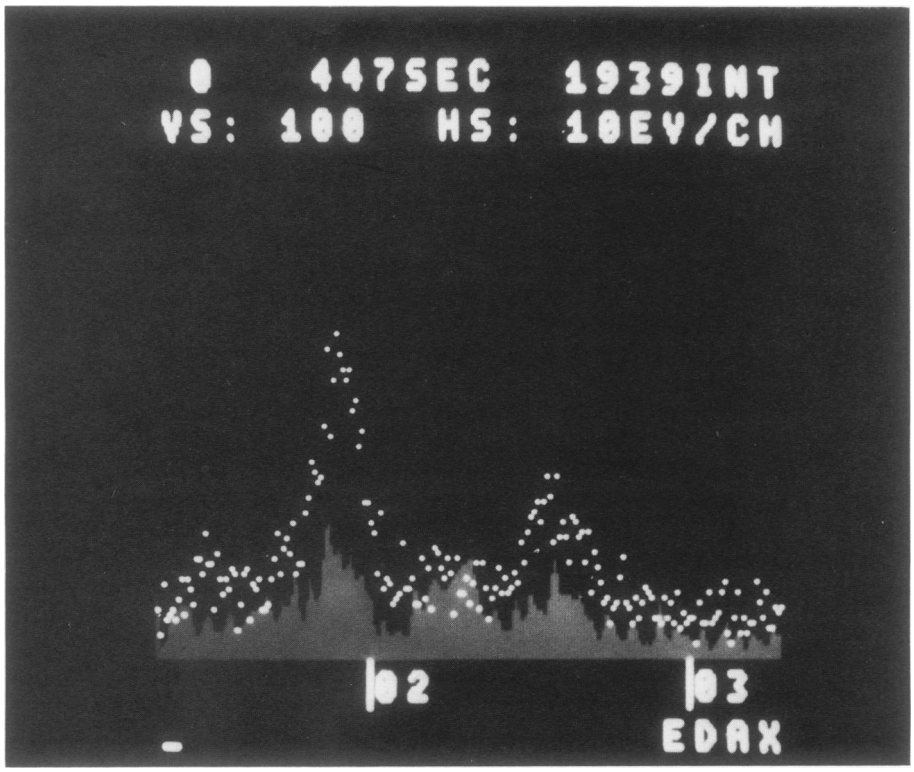

Figure 13—Display of energy dispersion analysis for ruthenium in ruthenium red-stained glycocalyx from a section through a blue area (*gray bars*) and an adjacent white area (*white dots*) from the same pig.

Figure 14—Injured endothelial cell (*E*) from a blue area. Cytoplasm is electron translucent and contains scattered membrane fragments (*arrows*) and large vacuoles (*V*). Nucleus (*N*) is dense and crenated. (Lead citrate and uranyl acetate, × 14,500)

Figure 15—Electron-dense degranulated cell (*C*) overlying gap between two normal endothelial cells. Appearance suggests that it is either a portion of a degenerate endothelial cell or, alternatively, an attenuated degranulated platelet. (Lead citrate and uranyl acetate, × 19,100)

Figure 16—Scanning electron micrograph of endothelial surface from a blue area showing microthrombus consisting of platelets (*P*), fibrin strand (*F*), and adherent erythrocytes (*RC*) overlying damaged endothelium (*E*), which appears to be lifting (*arrows*). (× 2800)

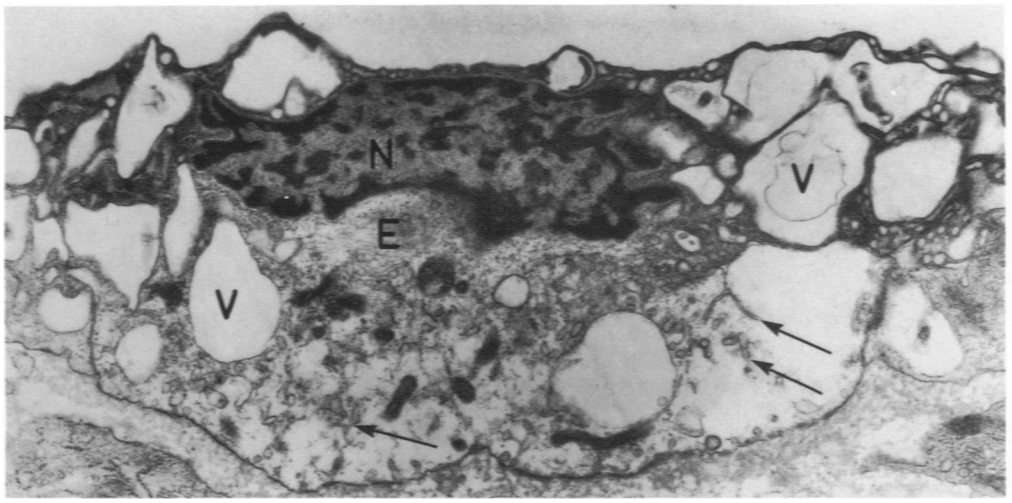

14

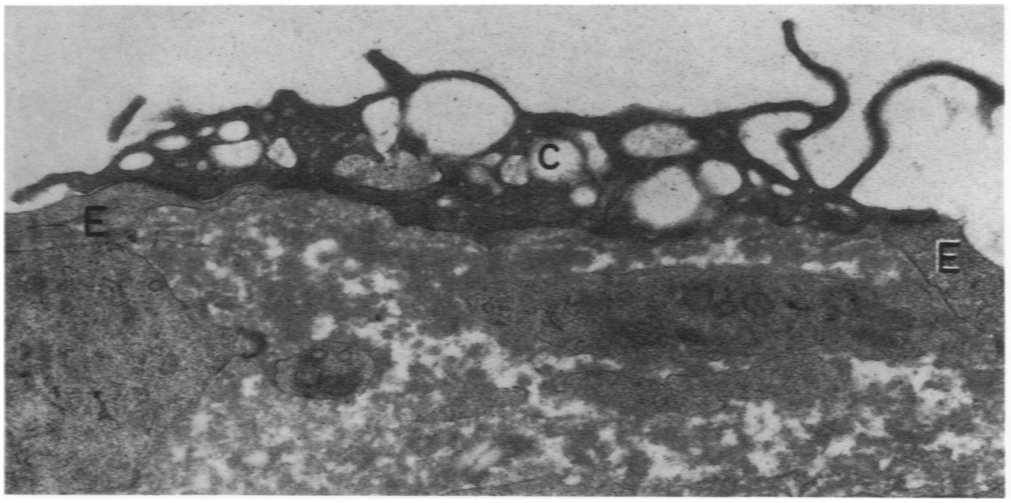

15

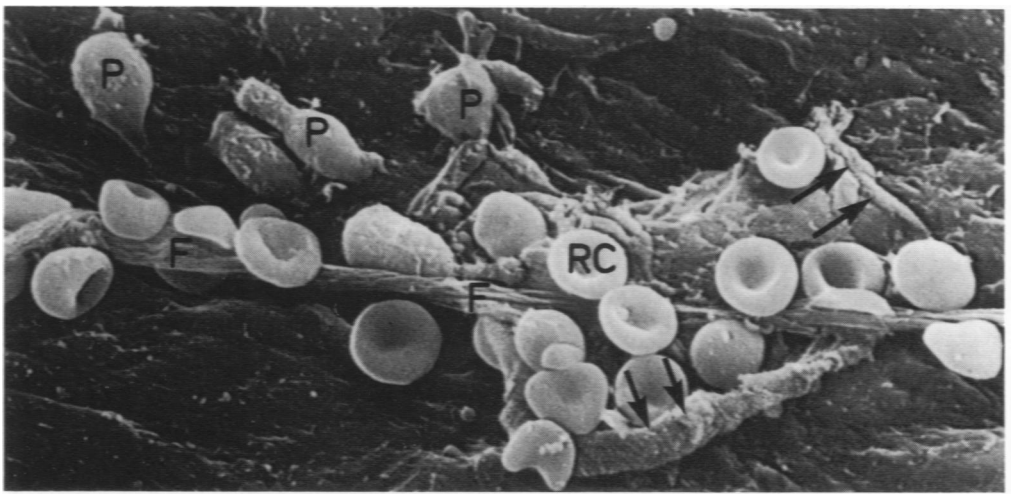

16

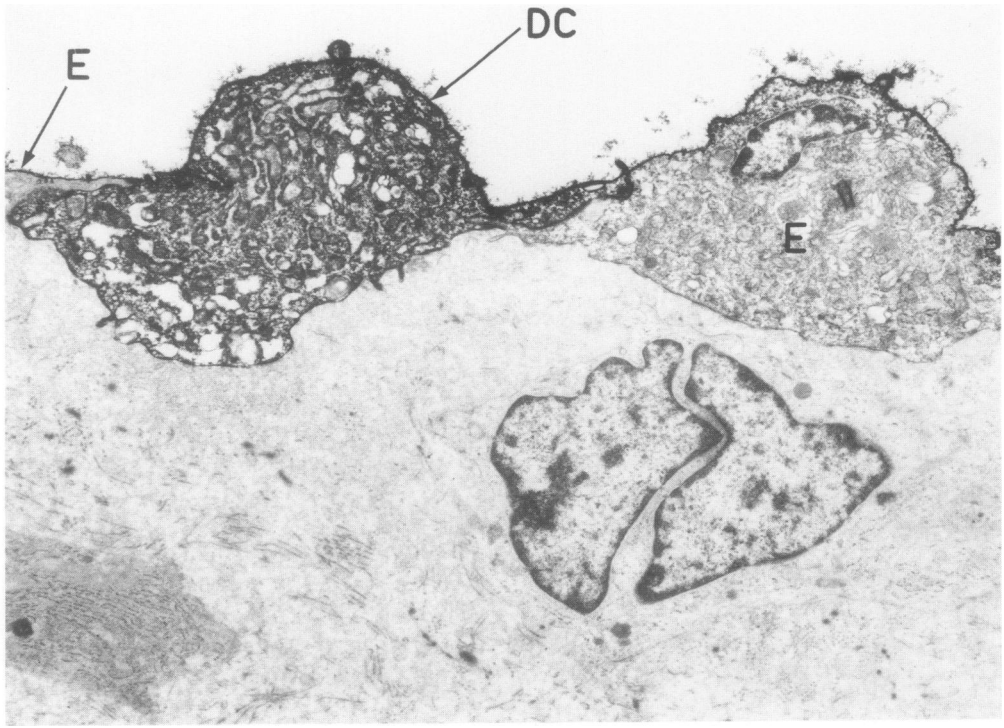

17

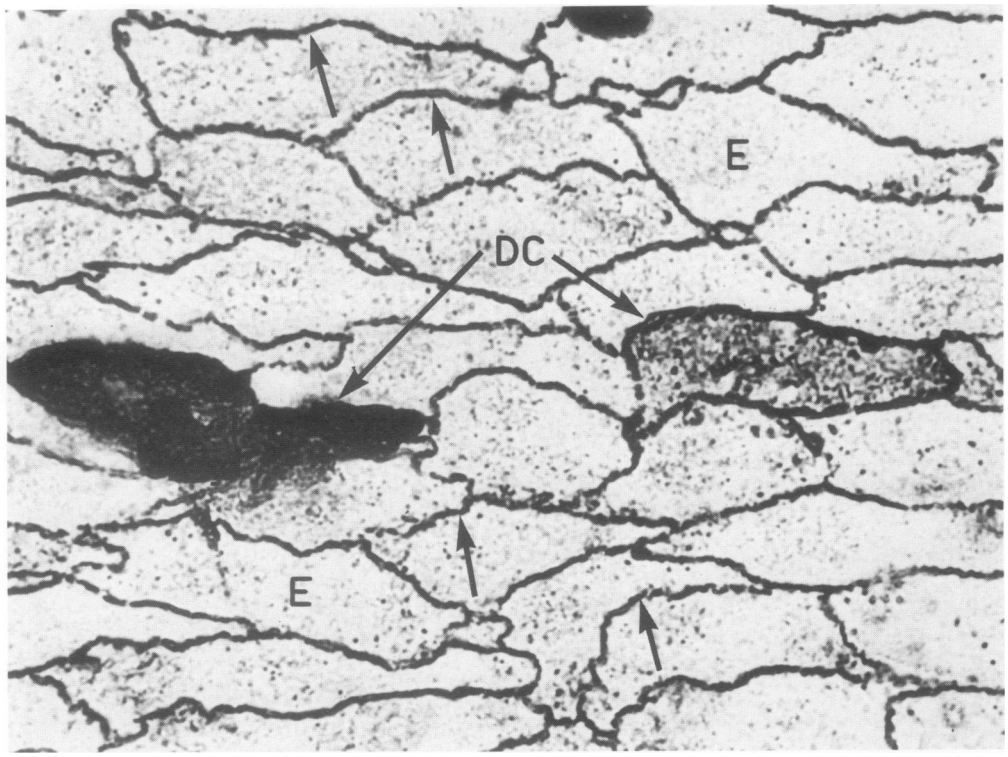

18

Figure 17—Transmission electron micrograph of endothelium from a blue area showing uptake of ruthenium red by an injured or dying endothelial cell (*DC*). Adjacent healthy endothelial cells (*E*) do not take up stain. (Ruthenium red block-stained, × 7600) **Figure 18**—Light micrograph of silver-nitrate-stained Hautchen preparation of endothelium from a blue area showing typical "pavement" appearance. Normal endothelial cells (*E*) are demarcated by silver-stained borders (*arrows*) Injured and dead cells show intense uptake of silver stain (*DC*). (× 4500)